Photodetachment cross section of H^- in electric and magnetic fields with any orientation

Z. Y. Liu, D. H. Wang, and S. L. Lin
Department of Physics, Shandong Normal University, Jinan 250014, China

W. Z. Shi
Department of Physics, Zhengzhou University, Zhengzhou 450052, China

(Received 1 April 1996)

In this paper we obtain the closed classical orbits of the detached electron from H^- in electric and magnetic fields with any orientation that lies in three-dimensional space. Using closed-orbit theory, we calculated the photodetachment cross section of H^-, which shows oscillations. These oscillations are correlated with three-dimensional closed orbits. Finally, we discuss the similarities and differences between the case of $\alpha=\pi/2$ and $\alpha\neq\pi/2$ (α is the angle between the electric and magnetic fields). [S1050-2947(96)05311-5]

PACS number(s): 32.80.Gc, 32.80.Fb, 03.65.Sq

I. INTRODUCTION

In the past few years, the photodetachment cross section of H^- in external electric or magnetic fields has been studied by many researchers [1–4]. Oscillations in the photodetachment cross section have been observed in experiments or predicted theoretically. Large oscillations in parallel electric and magnetic fields were predicted quantum mechanically by Du [3], and were correlated with closed classical orbits given by Peters, Jaffe, and Delos [2]. Quantum-mechanical and closed-orbit results describing the oscillations in crossed electric and magnetic fields were given by Peters and Delos [1], who derived a general formula for the photodetachment cross section of H^- in electric and magnetic fields with any orientation. The general formula displays that the cross section is a smooth background plus a sum of sinusoidal fluctuations:

$$\sigma(E)=\sigma_0(E)+\sum_{j=0}^{n}\sigma_{\mathrm{ret}}^{j}(E), \tag{1}$$

where σ_0 is the cross section in the absence of fields. The sum is over all closed classical orbits, $\sigma_{\mathrm{ret}}^{j}(E)$ is the oscillatory contribution to the cross section arising from the jth closed orbits, and is given by Peters and Delos in the following way:

$$\sigma_{\mathrm{ret}}^{j}(E)=-\frac{32\pi^2E_p}{c}\sum_j\ \frac{1}{r_{\mathrm{out}}}\left|\frac{J_j(t_0)}{J_j(t_{\mathrm{ret}})}\right|^{1/2}I_{l=1}^2 \times[\chi(\theta_{\mathrm{out}}^{j},\phi_{\mathrm{out}}^{j})\chi(\theta_{\mathrm{ret}}^{j},\phi_{\mathrm{out}}^{j})]\sin\left[S_j(t_{\mathrm{ret}})-\mu_j\frac{\pi}{2}\right]. \tag{2}$$

The sum is over all closed orbits for a given energy E. E_p is the photon energy, which is equal to the energy E of the detached electron plus the binding energy E_b ($E_p=E_b+E$). The factor $I_{l=1}$ is a radial dipole integral between the initial state (s state) and the outgoing wave state (p state). $\chi(\theta,\phi)$ is the angular distribution of the outgoing waves (according to the polarization of vector of the laser field), and is given by the following expressions (assuming that the light is polarized linearly in the x, y, or z direction):

$$\chi_x(\theta,\phi)=\frac{1}{\sqrt{4\pi}}\sin\theta\cos\phi,$$

$$\chi_y(\theta,\phi)=\frac{1}{\sqrt{4\pi}}\sin\theta\cos\phi,$$

$$\chi_z(\theta,\phi)=\frac{1}{\sqrt{4\pi}}\cos\theta. \tag{3}$$

The angles $\{\theta_{\mathrm{out}}^{j},\phi_{\mathrm{out}}^{j}\}$ and $\{\theta_{\mathrm{ret}}^{j},\phi_{\mathrm{ret}}^{j}\}$ refer to the outgoing and returning directions of the jth closed orbit. $J_j(t)$ is the Jacobian of the jth closed orbit, representing the divergence of adjacent trajectories in time. Thus $1/r_{\mathrm{out}}^2|J_j(t_0)/J_j(t_{\mathrm{ret}})|$ is the classical density of the jth closed orbit. S_j is the classical action of the jth closed orbit starting and ending at the origin and μ_j is the Maslov index. [For more details about $\sigma_{\mathrm{ret}}^{j}(E)$, refer to Ref. [1].]

In Sec. II we discuss the closed orbits of H^- in electric and magnetic fields with any orientation. Calculations show that the closed orbits have an orderly pattern: at any given energy, there is always one closed orbit, and a set of boundary energies exists. At each boundary energy, one additional closed orbit is created, and with the slightest increase of energy, the newly created closed orbit splits into two closed orbits. For each closed orbit, we calculate the following quantities: (i) the classical action S_j, which determines the phase of the returning wave relative to the outgoing wave; (ii) the Maslov index μ_j, which is the number of caustics and foci through which the jth closed orbit passes; (iii) the classical density of the neighbors of each closed orbit, which determines the amplitude of each returning wave.

In Sec. III the semiclassical photodetachment cross section is calculated using the classical results of Sec. II, and

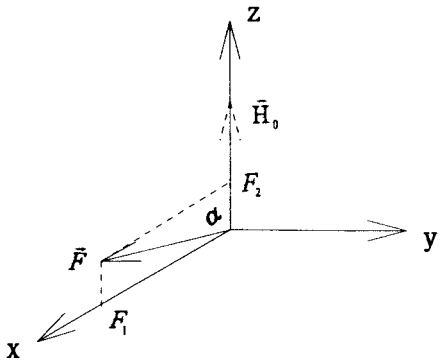

FIG. 1. The magnetic field $\vec{H}_0$ points in the positive z direction, and the electric field $\vec{F}$ lies in the x-z plane. The angle between the electric and magnetic fields is denoted by α. The x or z components of the electric field $\vec{F}$ are denoted by F_1 or F_2 (H_0=0.6 T, F=18 V/cm).

oscillations are displayed in the cross section. In Sec. IV, we compare the similarities and differences of closed orbits between $\alpha=\pi/2$ and $\alpha\neq\pi/2$ (α is the angle between the electric and magnetic fields) and discuss their influences upon the cross section. Atomic units are used throughout this paper unless otherwise noted.

II. CLASSICAL MOTION

In this section, we examine the classical trajectories for an electron in the electric and magnetic fields with any orientation. Let the magnetic field $\vec{H}_0$ point in the positive z direction and the electric field $\vec{F}$ lie in the x-z plane. The angle between the electric and magnetic fields is denoted by α (Fig. 1). It is convenient to separate the electric field $\vec{F}$ into two components: one is F_1 in the positive x direction, and the other is F_2 in the positive z direction. F_1 and F_2 are given in the following way:

$$\begin{cases} F_1 = F\ \sin\alpha, \\ F_2 = F\ \cos\alpha. \end{cases} \tag{4}$$

With this done, the motion of the electron can be separated into a motion of uniform acceleration along the z axis and a motion in the x-y plane. For closed orbits, the z component P_{z_0} of the initial momentum $\vec{P}$ must be greater than zero. Motion in the x-y plane is a trochoid: a circular motion about a center superposed upon a translational motion along the y axis. For closed orbits, the linear speed [or the ''$\vec{E}\times\vec{H}$ drift'' velocity $c(F_1/H_0)$] must be less than the circular speed.

A. Families of trajectories and returning orbits

Classically, once the electron is photodetached from H^- by the laser light, it will have a uniform acceleration motion along the z axis, and exhibit a trochoidal motion in the x-y plane: circular cyclotron motion at constant speed relative to a center moving at the fixed $\vec{E}\times\vec{H}$ drift velocity. The motion equation of the electron in the electric and magnetic fields is described in many textbooks [5]:

$$\frac{d\vec{p}}{dt} = -\left(\vec{F} + \frac{\vec{V}}{c}\times\vec{H}_0\right). \tag{5}$$

It is convenient to define a set of scaled variables as was done by Peters and Delos [1] in crossed electric and magnetic fields:

$$q' = \frac{\omega_B^2}{F_1}\, q,$$

$$t' = \omega_B t,$$

$$p' = \frac{\omega_B}{F_1}\, p, \tag{6}$$

where ω_B is the electron's cyclotron frequency defined by

$$\omega_B = \frac{H_0}{C}. \tag{7}$$

Units of time are chosen such that one cyclotron period is 2π units and units of length are chosen such that the drift velocity $[c(F_1/H_0)]$ is 1. In these units, the position as a function of time, i.e., the solution of Eq. (5), is

$$\chi(t) = \sqrt{2\varepsilon}[\sin(t+\varphi) - \sin\varphi],$$

$$y(t) = -\sqrt{2\varepsilon}[\cos(t+\varphi) - \cos\varphi] - t,$$

$$z(t) = -\frac{1}{2}\frac{F_2}{F_1}\, t^2 + p_{z_0} t. \tag{8}$$

These equations are the parametric representations of the motion of the electron: circular motion about a center superposed upon a translational motion in the x-y plane and a uniform acceleration motion along the z axis. The radius of the circular motion is given by the quantity $\sqrt{2\varepsilon}$, which is the speed of the circular motion; ε is that part of the kinetic energy associated with the circular motion. The translation of the electron (''$\vec{E}\times\vec{H}$ drift'' velocity) has a velocity $-(F_1/\omega_B)$, which in scaled units has a fixed value of -1.

The initial conditions on the trajectories follow from the fact that the electron is detached from H^- by a laser: all electrons begin at $\{x=0, y=0, z=0\}$ going outward in all directions, all at the same speed determined by the photon energy. From Eq. (8), we can conclude for the closed orbits: (i) at $\alpha\neq\pi/2$, the electric field $\vec{F}$ has one component F_2 in the z axis, so only when P_{z_0} is greater than zero is it possible for the electron to return to the origin; (ii) at $\alpha\neq\pi/2$, the motion of electron in the x-y plane is the same as that at $\alpha=\pi/2$. Peters and Delos [1] have pointed out that if the ''$\vec{E}\times\vec{H}$ drift'' velocity is less than the circular speed, the electron may return to the origin. Therefore, at $\alpha\neq\pi/2$, the closed orbits must be in three-dimensional space.

Figure 2 shows a family of electron orbits for three different values of angle α at low energy E. There is one closed orbit that allows the electron to return to the origin. After the trajectories leave the origin, they diverge from each other. At the caustics or boundaries between classically allowed and forbidden regions, the trajectories cross back over each other

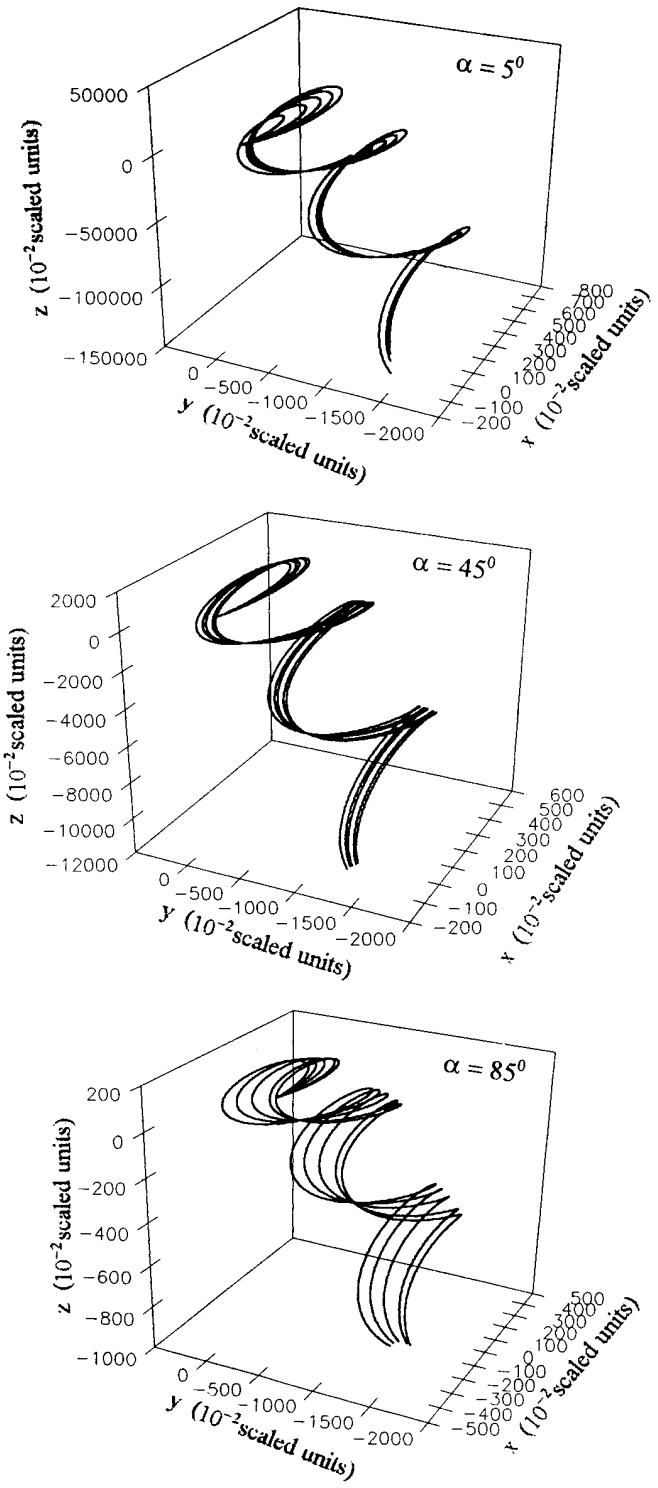

FIG. 2. Family of trajectories representing electrons moving away from the H atom. As the trajectories leave the origin, they diverge from one another. The trajectories continue until they cross back over each other, giving rise to a caustic. After being turned back by the fields, the trajectories pass close to the origin and then continue until they pass through a focus at $t=1$ cyclotron time, where they converge. This process repeats itself.

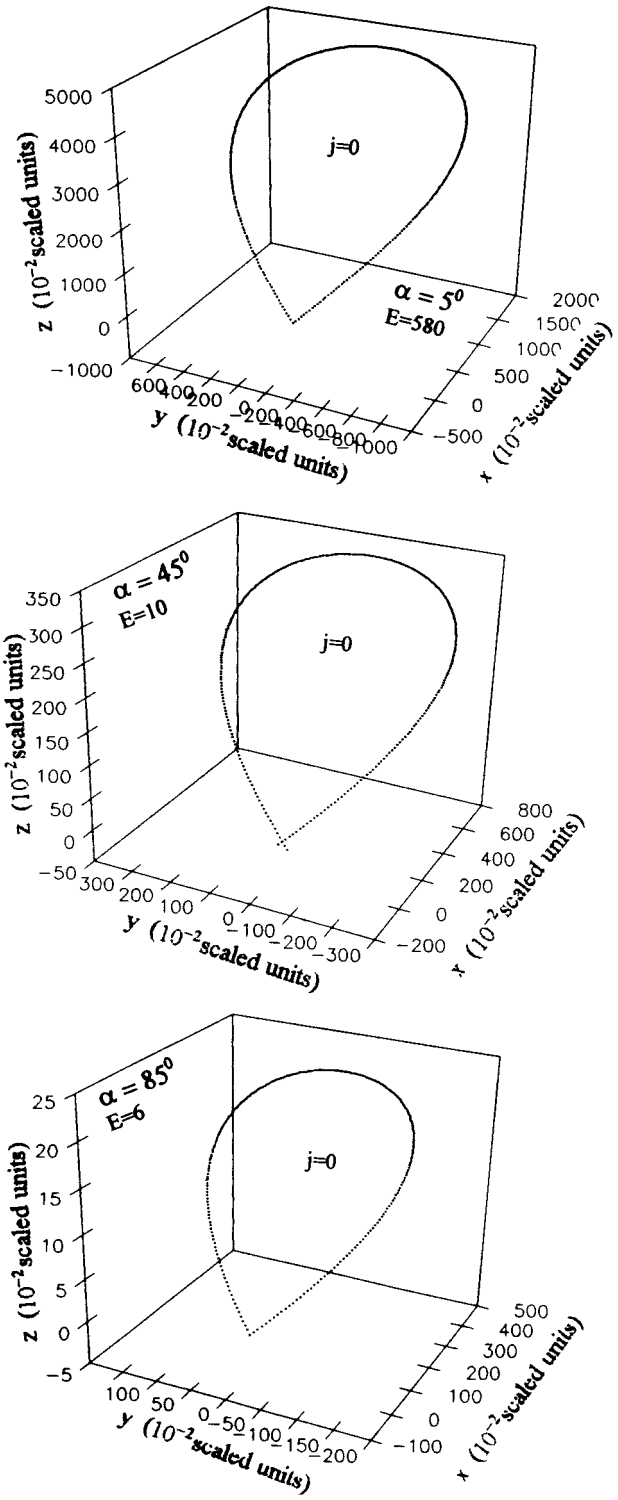

FIG. 3. The closed orbits at low scaled energy E, which are labeled by $j=0$.

and then, after being turned back by the fields, they pass close to the origin. The trajectories continue until they pass through a focus at $t=1$ cyclotron time, where they converge. This process repeats itself.

At low energy E there is only one closed orbit (Fig. 3). As we increase the scaled energy E to a value $E^{(b1)}$, Fig. 4 shows that a new closed orbit arises. This energy $E^{(b1)}$ is called the first boundary energy. With the increase of energy away from $E^{(b1)}$, the newly arising closed orbit splits into a pair (Fig. 5). As we continue to increase the energy to the second boundary energy $E^{(b2)}$, Fig. 6 shows that again a new closed orbit is created. As we continue to increase the energy

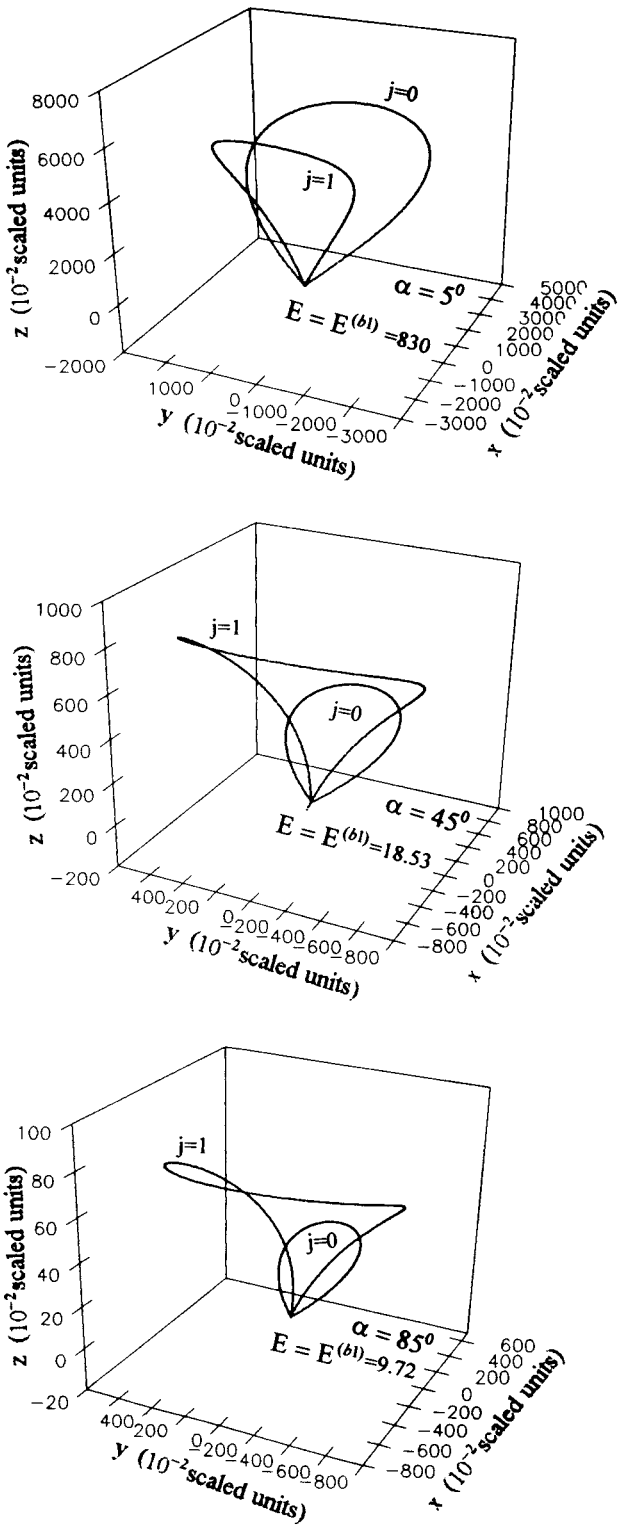

FIG. 4. The energy increases to the first boundary energy $E=E^{(b1)}$, at which a new closed orbit is created. The newly created closed orbit is called the first boundary orbit, labeled by $j=1$. At the boundary energy, there are two closed orbits.

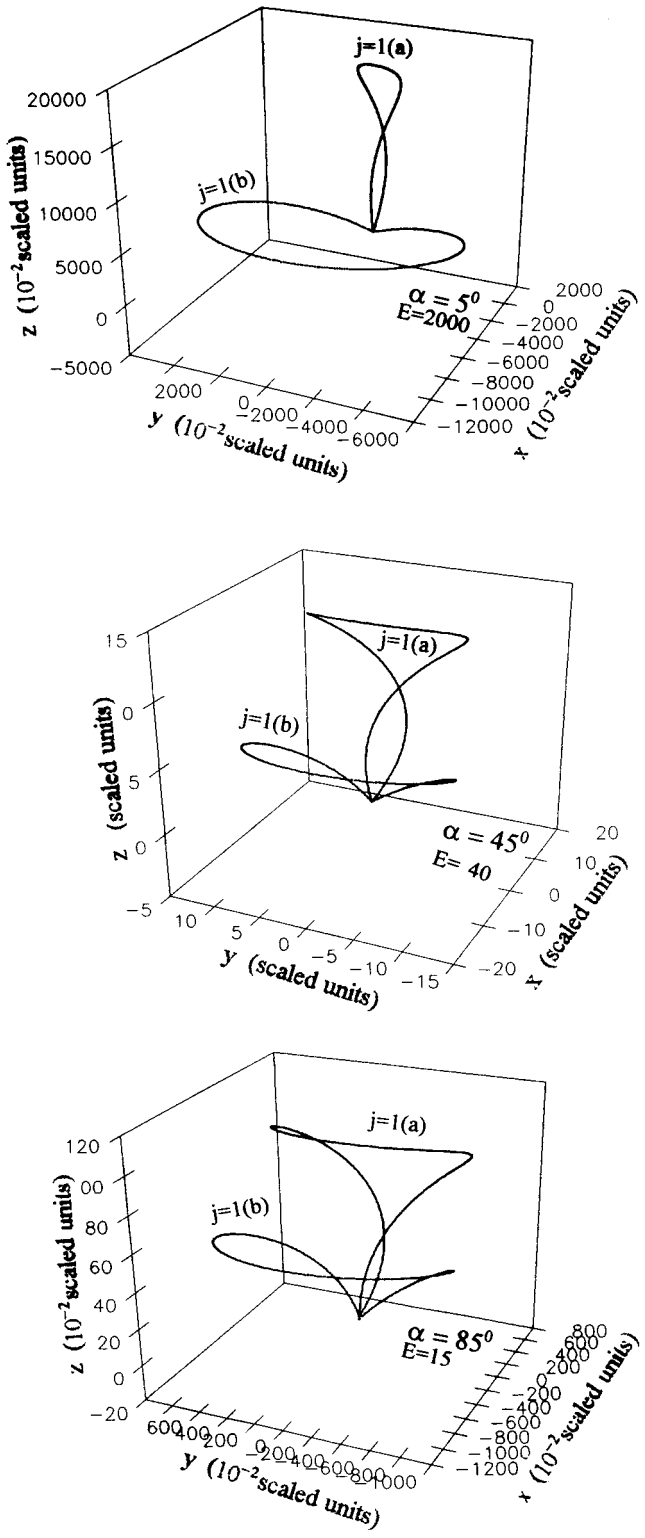

FIG. 5. As the scaled energy E increases from the first boundary energy $E^{(b1)}$, the newly created closed orbit separates into two closed orbits, which are labeled by $j=1(a)$ and $1(b)$. At this energy, there are three closed orbits, while the $j=0$ orbit is omitted.

away from $E^{(b2)}$, the newly created orbit then splits into a pair (Fig. 7). Thus, as the energy continues to increase, the number of the closed orbits increases steadily from 1 to 3 to 5, and so on. For any value of angle α, we conclude that at any given energy E there is at least one closed orbit. At each of a set of discrete boundary energies a new closed orbit is created. The newly created orbit separates into two closed orbits when the energy increases away from the boundary energy. For any given energy, which is not the boundary energy, there are $(2j+1)$ closed orbits.

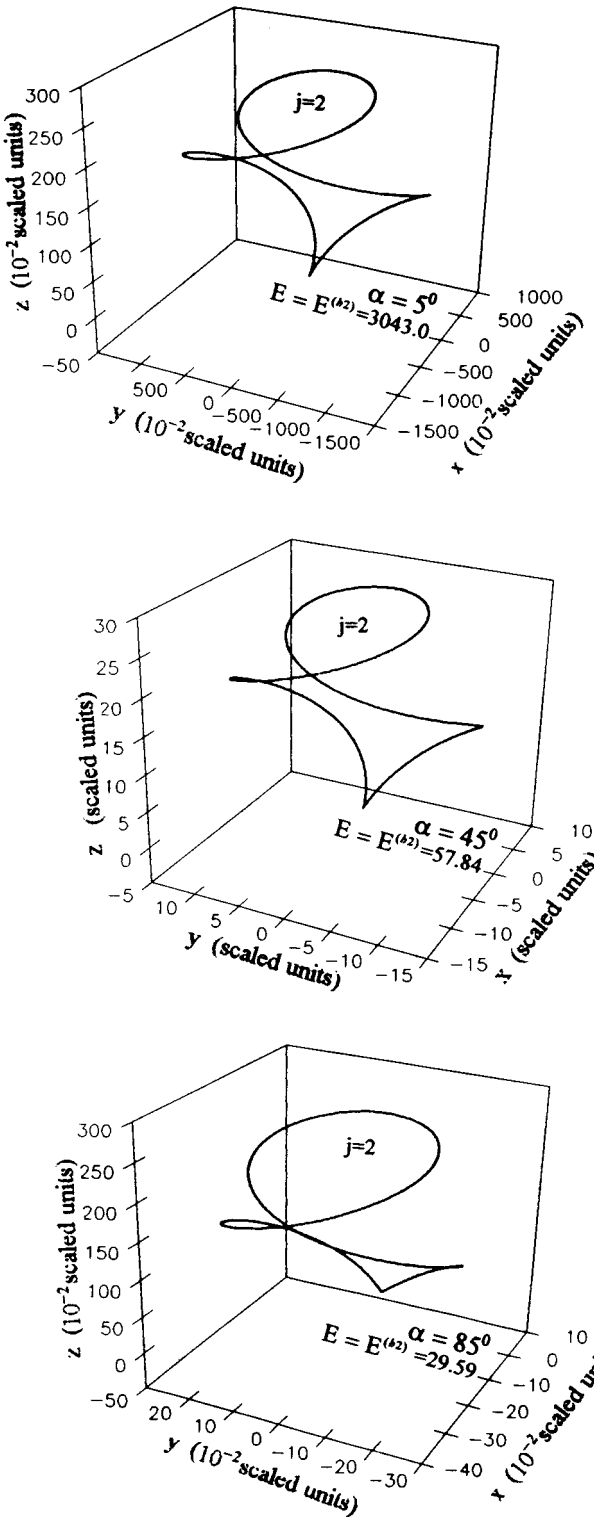

FIG. 6. The energy is increased to the second boundary energy $E=E^{(b2)}$, at which again a new closed orbit is created and labeled by $j=2$. At this energy, there are four closed orbits. The $j=0,1$ orbits are omitted.

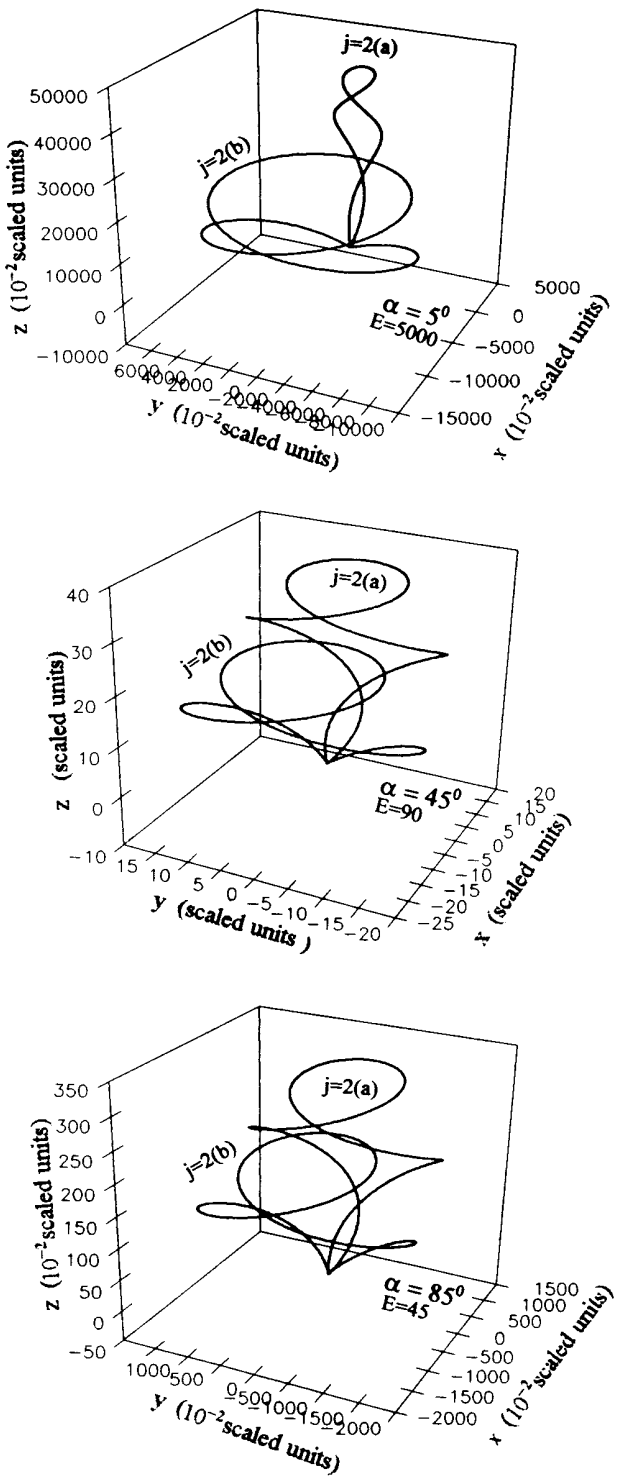

FIG. 7. As the scaled energy E is larger than the second boundary energy $E^{(b2)}$, the second boundary orbit splits into two closed orbits, which are labeled by $j=2(a)$ and $2(b)$. There are five closed orbits at this energy. The $j=0,1$ and $b=1,2$ orbits are omitted.

In the following parts of this section, we will give the quantitative analysis of these facts. For any given closed orbit, we will give the formulas for the classical action, density, and Maslov index.

B. Closed orbits—quantitative theory

1. Hamiltonian equation of motion

The Hamiltonian of an electron in the electric and magnetic fields is given by

$$H=\frac{1}{2}\left[\vec{P}-\frac{\vec{A}}{c}\right]^2+F_1\chi+F_2z, \tag{9}$$

where $-F_1\chi-F_2z$ is the scalar potential of the electric field; $\vec{F},\vec{A}$ is the vector potential of the magnetic field $\vec{H}_0$, which is defined by

$$\vec{A}=H_0x\vec{j}, \tag{10}$$

where $\vec{j}$ is a unit vector directed along the y axis. Defining the following quantities

$$\varepsilon=\tfrac{1}{2}P_x^2+\tfrac{1}{2}\omega_B^2\left[x+\frac{1}{\omega_B}\left(P_y+\frac{F_1}{\omega_B}\right)\right]^2 \tag{11}$$

and

$$H_z=\tfrac{1}{2}P_z^2+F_2z, \tag{12}$$

the Hamiltonian can be reexpressed by

$$H=\varepsilon-\frac{F_1}{\omega_B}P_y-\frac{1}{2}\left(\frac{F_1}{\omega_B}\right)^2+H_z. \tag{13}$$

It is easy to prove that ε, P_y, and H_z are independently conserved. By making use of the scale change defined by Eq. (6) and

$$H'=\left(\frac{F_1}{\omega_B}\right)^{-2}H, \tag{14}$$

after omitting the primes, the Hamiltonian is given by

$$H=\varepsilon-P_y-\tfrac{1}{2}+H_z, \tag{15}$$

where

$$\varepsilon=\tfrac{1}{2}P_x^2+\tfrac{1}{2}[x+(P_y+1)]^2, \tag{16}$$

and

$$H_z=\tfrac{1}{2}P_z^2+\frac{F_2}{F_1}z. \tag{17}$$

So the dependence of the Hamiltonian on the field strength is removed, but the dependence on the angle α still remains.

As stated earlier, after detaching from H^-, the electron moves away from the origin in any direction with the fixed initial momenta $\{P_{x_0},P_{y_0},P_{z_0}\}$. Now, with the Hamiltonian of the electron known, we obtain that the electron's velocity with time is described by the following expressions:

$$P_x(t)=\dot{x}(t),$$

$$P_y(t)=\dot{y}(t)-x(t)=P_{y_0},$$

$$P_z(t)=\dot{z}(t). \tag{18}$$

From Eqs. (8) and (18), we obtain that φ is related to ε in the following way:

$$\sin\varphi=\frac{1}{\sqrt{2\varepsilon}}(P_{y_0}+1),$$

$$\cos\varphi=\frac{1}{\sqrt{2\varepsilon}}P_{x_0}. \tag{19}$$

Equation (19) implies that there is a relationship between the initial direction of propagation of the electron and the radius of the circular motion.

2. Initial coordinates for closed orbits

From energy conservation and Eqs. (15)–(17), we must have

$$E=\varepsilon-P_{y_0}-\tfrac{1}{2}+\tfrac{1}{2}P_{z_0}^2 \tag{20}$$

and

$$\varepsilon=\tfrac{1}{2}P_{x_0}^2+\tfrac{1}{2}[P_{y_0}+1]^2. \tag{21}$$

For closed orbits, we must have the following facts:

$$x(t_{\rm ret})=0, \tag{22a}$$

$$y(t_{\rm ret})=0, \tag{22b}$$

$$z(t_{\rm ret})=0, \tag{22c}$$

where $t_{\rm ret}$ is the returning time. With the help of Eqs. (8), Eq. (22a) gives the returning time $t_{\rm ret}$,

$$t_{\rm ret}=-2\varphi+(2j+1)\pi, \tag{23}$$

where j is an integer. Equations (22b) and (22c) can give the following conditions:

$$\cos\varphi+\frac{1}{\sqrt{2\varepsilon}}\varphi-\frac{1}{\sqrt{2\varepsilon}}\left(j+\frac{1}{2}\right)\pi=0, \tag{24}$$

and

$$P_{z_0}=\frac{1}{2}\frac{F_2}{F_1}t_{\rm ret}. \tag{25}$$

Equations (23)–(25) also imply

$$t_{\rm ret}=2\sqrt{2\varepsilon}\cos\varphi \tag{26a}$$

and

$$P_{z_0}=\frac{F_2}{F_1}P_{x_0}. \tag{26b}$$

Since the returning time $t_{\rm ret}$ is positive, Eqs. (19) and (26) display that $\cos\varphi$ and then P_{x_0} and P_{z_0} must be positive, and Eq. (26b) also implies that for closed orbits the electron must begin its motion in the x-z plane against the electric field $\vec{F}$. By solving Eq. (21), we obtain

$$P_{x_0}=[2\varepsilon-(P_{y_0}+1)^2]^{1/2}. \tag{27}$$

Some additional manipulations reduce Eqs. (23)–(25) to an equation involving only ε and the fixed total energy E. By removing φ and $t_{\rm ret}$ from these equations, we obtain

$$[2\varepsilon-(P_{y_0}+1)^2]^{1/2}-\cos^{-1}\left[\frac{P_{y_0}+1}{\sqrt{2\varepsilon}}\right]=j\pi,$$

$$L(\varepsilon)=j\pi, \tag{28}$$

where $L(\varepsilon)$ is the left-hand side of Eq. (28). By a long tedious deduction we obtain $P_{y_0}+1$ from energy conservation and Eqs. (26b) and (27). For $E\leqslant E_\alpha$,

$$P_{y_0}+1=-\left(\frac{F_1}{F_2}\right)^2+\left[2\varepsilon\left(\frac{F}{F_2}\right)^2-2E\left(\frac{F_1}{F_2}\right)^2+\left(\frac{F}{F_2}\right)^2\left(\frac{F_1}{F_2}\right)^2\right]^{1/2},\quad \varepsilon_1\leqslant\varepsilon\leqslant\varepsilon_2 \tag{29a}$$

and for $E\geqslant E\alpha$,

$$P_{y_0}+1=\begin{cases}-\left(\frac{F_1}{F_2}\right)^2+\left[2\varepsilon\left(\frac{F}{F_2}\right)^2-2E\left(\frac{F_1}{F_2}\right)^2+\left(\frac{F}{F_2}\right)^2\left(\frac{F_1}{F_2}\right)^2\right]^{1/2}, & \varepsilon_3\leqslant\varepsilon\leqslant\varepsilon_2,\\ -\left(\frac{F_1}{F_2}\right)^2-\left[2\varepsilon\left(\frac{F}{F_2}\right)^2-2E\left(\frac{F_1}{F_2}\right)^2+\left(\frac{F}{F_2}\right)^2\left(\frac{F_1}{F_2}\right)^2\right]^{1/2}, & \varepsilon_3\leqslant\varepsilon\leqslant\varepsilon_1,\end{cases} \tag{29b}$$

where $E_\alpha,\varepsilon_1,\varepsilon_2,\varepsilon_3$ are given in the following expressions:

$$E_\alpha=\frac{1}{2\cos^4\alpha},$$

$$\varepsilon_1=\frac{(\sqrt{2E}-1)^2}{2},$$

$$\varepsilon_2=\frac{(\sqrt{2E}+1)^2}{2},$$

$$\varepsilon_3=\left(\frac{F_1}{F}\right)^2E-\frac{1}{2}\left(\frac{F_1}{F_2}\right)^2=E\,\sin^2\alpha-\tfrac{1}{2}\,\tan^2\alpha\leqslant\varepsilon_1. \tag{30}$$

Given the total energy E, Eqs. (28)–(30) can be used to determine the value of ε_j for which there is a closed orbit. Substituting ε_j into Eq. (29a) or (29b) according to the given energy E, we can obtain the momentum P_{y_0} or P_j for that closed orbit. With ε_j and P_j determined for that closed orbit, Eqs. (26b) and (27) give the values of P_{x_0} and P_{z_0}. The initial conditions for that closed orbit are then known.

3. Boundary orbits

In this part, we will determine the number of closed orbits existing at any given energy and the boundary energies where new closed orbits appear. For three different values of angle α, the left-hand side $L(\varepsilon)$ of Eq. (28) has been plotted at several values of the total energy E as a function of ε (Fig. 8). The right-hand side has also been plotted for $j=0$ and 1. For any given energy E, $L(\varepsilon)$ has a single maximum. Since the maximum of $L(\varepsilon)$ is greater than zero at all energies, one solution always exists for $j=0$. At low energy E, the maximum of $L(\varepsilon)$ is less than π, so no solutions exist for $j\geqslant1$. At large enough values of E, $L(\varepsilon)$ has a maximum that is greater than π. In this case, there are two roots to Eq. (28) for $j=1$, and therefore there are two closed orbits, which are labeled $j=1(a)$ and $1(b)$, respectively.

There is a set of energies $E^{(b_j)}$ that are called boundary energies. At each energy $E^{(b_j)}$, the curve of $L(\varepsilon)$ is tangent to the line defined by $j\pi$. So at this energy a new closed orbit is formed, and this newly formed closed orbit is called the jth boundary orbit. By differentiating $L(\varepsilon)$ with respect to ε, holding E fixed, we find that the maximum of $L(\varepsilon)$ occurs when

$$(2\varepsilon_b-1)P_{y_0}(\varepsilon_b)=2E, \tag{31}$$

where $P_{y_0}(\varepsilon_{(b)})=-(F/F_2)^2+[2\varepsilon(F/F_2)^2-2E(F_1/F_2)^2+(F/F_2)^2(F_1/F_2)^2]^{1/2}$.

Substituting this value for $P_{y_0}(\varepsilon_b)$ obtained from Eq. (31) into Eq. (28), we solve for the boundary energy $E^{(b_j)}$ and $\varepsilon^{(b_j)}$ numerically. Table I gives some boundary energies for three different values of angle α. Figure 9 shows the curves of the boundary energies $E^{(b1)}$ and $E^{(b2)}$ as a function of angle α. It is obvious that the smaller the angle α, the lower the boundary energies. This fact implies that at a given energy E, there may be more closed orbits for smaller values of angle α.

4. The Jacobian $J(t)$

The ratio of Jacobians $[J(t_0)/J(t_{\rm ret})]$ in the oscillatory cross section [Eq. (2)] represents the divergence of trajectories with time. In the following part we will give the calculation of the ratio of Jacobians.

The Jacobian is given by[1]:

$$J(t)=\frac{\partial(x,y,z)}{\partial(t,\theta_{\rm out},\phi_{\rm out})}. \tag{32}$$

The coordinates $\{t,\theta_{\rm out},\phi_{\rm out}\}$ are the coordinates for the family of trajectories. As the electron propagates into the external region, the symmetry is broken by the external fields. Equation (8) shows that $\{t,\sqrt{2\varepsilon},\varphi\}$ becomes the convenient variables to express the motion of the electron in the electric and magnetic fields. Therefore, we can rewrite the Jacobian in the following way:

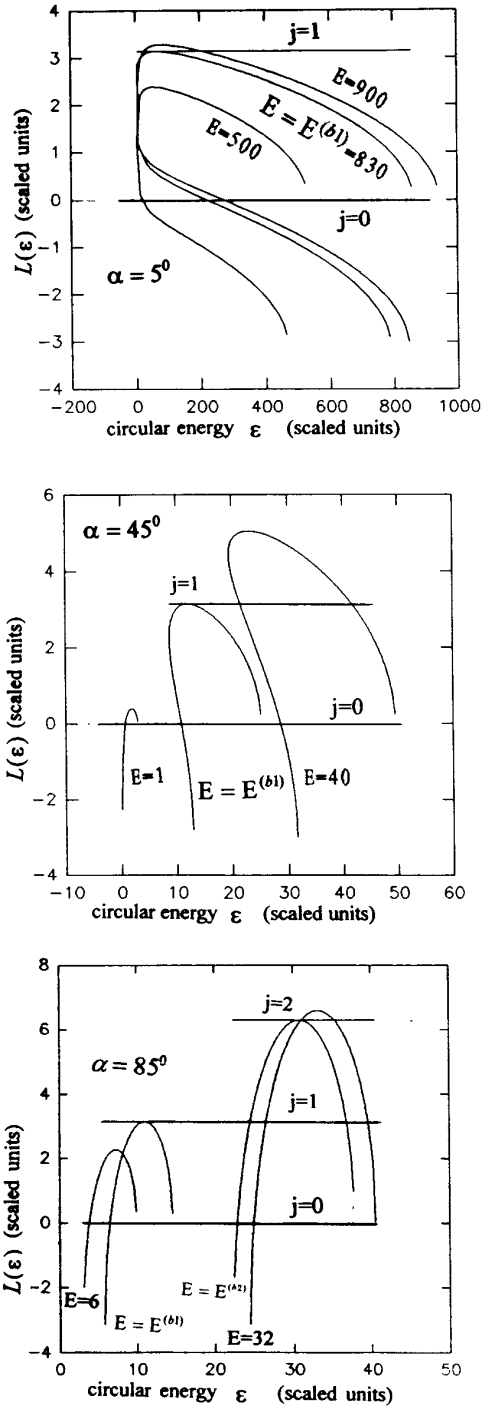

FIG. 8. Graphical solutions of Eq. (28). The curves represent the left-hand side of Eq. (28), and the horizontal lines are the right-hand side of Eq. (28). The intersections of the curves and lines are the solution of Eq. (28). For any given energy larger than zero, one solution always exists for Eq. (28), i.e., one closed orbit always exists. This solution is labeled by $j=0$. At low energies, the maximum of $L(\varepsilon)$ is less than π, so there are no solutions for $j \geqslant 1$. As the energy increases to the first boundary energy $E^{(b1)}$, the maximum point of $L(\varepsilon)$ is tangent to the horizontal line defined by $j\pi$ with $j=1$ and then a new closed orbit is created. As the energy continues to increase from $E^{(b1)}$, there are two intersections of the curve with the horizontal line $j=1$, and two solutions to Eq. (28) exist. These two solutions correspond to two closed orbits, which have circular energies $\varepsilon_1(a)$ and $\varepsilon_1(b)$, respectively.

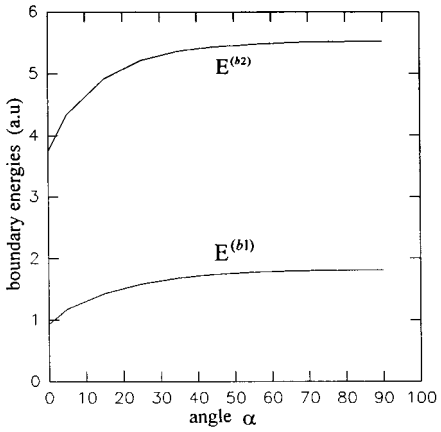

FIG. 9. The curves of the first and second boundary energies as functions of the angle α. As the α becomes small, the boundary energies decrease.

$$J(t)=\frac{\partial(t,\sqrt{2\varepsilon},\varphi)}{\partial(t,\theta_{\text{out}},\phi_{\text{out}})}\frac{\partial(x,y,z)}{\partial(t,\sqrt{2\varepsilon},\varphi)}, \tag{33a}$$

$$=g(\varepsilon,\varphi)\begin{vmatrix} \frac{\partial x}{\partial t} & \frac{\partial x}{\partial\sqrt{2\varepsilon}} & \frac{\partial x}{\partial\varphi} \\ \frac{\partial y}{\partial t} & \frac{\partial y}{\partial\sqrt{2\varepsilon}} & \frac{\partial y}{\partial\varphi} \\ \frac{\partial z}{\partial t} & \frac{\partial z}{\partial\sqrt{2\varepsilon}} & \frac{\partial z}{\partial\varphi} \end{vmatrix}. \tag{33b}$$

The quantity $g(\varepsilon,\varphi)$ is the first determinant in Eq. (33a). Peters and Delos [1] have pointed out that $g(\varepsilon,\varphi)$ is a geometrical factor, and is independent of time. From Eq. (8), a straightforward evaluation of the second determinant in Eq. (33b) gives the result:

$$J(t)=g(\varepsilon,\varphi)\left\{4\sqrt{2\varepsilon}\left(P_{z_0}-\frac{F_2}{F_1}t\right)\sin^2\frac{t}{2}\right.$$
$$+t\frac{\sqrt{2\varepsilon}}{P_{z_0}}2\sin\frac{t}{2}\left[2\left(\varepsilon-P_{y_0}-\frac{1}{2}\right)\cos\frac{t}{2}\right.$$
$$\left.\left.-2[2\varepsilon-(P_{y_0}+1)]^{1/2}\sin\frac{t}{2}\right]\right\}. \tag{34}$$

This is the Jacobian for any trajectory at any time. For closed orbits, the momentum in the z direction $P_{z_0}=1/2(F_2/F_1)t_{\text{ret}}$. If $t=t_0$ (initial time) or $t=t_{\text{ret}}$, x and z are small. So we can write the energy conservation in the following way:

$$E=\varepsilon_j-P_{y_0}-\tfrac{1}{2}+\tfrac{1}{2}P_{z_0}^2. \tag{35}$$

Then we can write the Jacobian for the jth closed orbit in the following expression:

$$J(t)=g(\varepsilon,\varphi)\left\{4\sqrt{2\varepsilon_j}\left(P_{z_0}-\frac{F_2}{F_1}t\right)\sin^2\frac{t}{2}+t\frac{\sqrt{2\varepsilon_j}}{P_{z_0}}2\sin\frac{t}{2}\left[(2E-P_{z_0}^2)^2\cos\frac{t}{2}-2[2\varepsilon_j-(P_{y_0}+1)]^{1/2}\sin\frac{t}{2}\right]\right\}. \quad (36)$$

This is the Jacobian calculated at either $t=t_0$ or $t=t_{\rm ret}$. At $t=t_0$ with t_0 small, expanding the trigonometric functions of Eq. (36) and keeping only the lowest order of t_0, we have that the Jacobian at $t=t_0$ is

$$J(t_0)=g\frac{\sqrt{2\varepsilon_j}}{P_{z_0}}t_0^2(2E). \quad (37)$$

At $t=t_{\rm ret}=-2\varphi+(2j+1)\pi$, we have

$$\cos\frac{t_{\rm ret}}{2}=(-1)^j\sin\varphi, \quad (38)$$

$$\sin\frac{t_{\rm ret}}{2}=(-1)^j\cos\varphi,$$

$$P_{z_0}-\frac{F_2}{F_1}t_{\rm ret}=-P_{z_0}.$$

With the help of Eq. (19) which give the definitions for $\sin\varphi$ and $\cos\varphi$, the Jacobian at $t=t_{\rm ret}$ becomes

$$J(t_{\rm ret})=g\frac{(2\varepsilon_j)^2}{P_{z_0}}\times4\left[1-\left(\frac{P_{y_0}+1}{\sqrt{2\varepsilon_j}}\right)^2\right]\left(\frac{P_{y_0}+1}{\sqrt{2\varepsilon_j}}\left[1+\frac{1}{2\varepsilon_j}\right]-\frac{1}{\sqrt{2\varepsilon_j}}\left\{2+\left(\frac{F_2}{F_1}\right)^2\left[1-\left(\frac{P_{y_0}+1}{\sqrt{2\varepsilon_j}}\right)^2\right]\right\}\right). \quad (39)$$

With $J(t_0)$ and $J(t_{\rm ret})$ obtained, we have the ratio of the Jacobians

$$\frac{J(t_0)}{J(t_{\rm ret})}=\frac{\sqrt{2\varepsilon_j}t_0^2(2E)}{(2\varepsilon_j)^2\times4\left[1-\left(\frac{P_{y_0}+1}{\sqrt{2\varepsilon_j}}\right)^2\right]\left(\frac{P_{y_0}+1}{\sqrt{2\varepsilon_j}}\left[1+\frac{1}{2\varepsilon_j}\right]-\frac{1}{\sqrt{2\varepsilon_j}}\left\{2+\left(\frac{F_2}{F_1}\right)^2\left[1-\left(\frac{P_{y_0}+1}{\sqrt{2\varepsilon_j}}\right)^2\right]\right\}\right)}. \quad (40)$$

Coming out of the scaled variables and making use of the following dimensionless variables:

$$\tilde{\nu}_j=\frac{F_1/\omega_B}{\sqrt{2\varepsilon_j}},$$

$$\nu_j=\frac{1}{\sqrt{2\varepsilon_j}}\left[P_{y_0}+\frac{F_1}{\omega_B}\right], \quad (41)$$

we rewrite Eq. (40) as

$$\frac{J(t_0)}{J(t_{\rm ret})}=\frac{\tilde{\nu}_j^2}{(F_1/\omega_B)^2}\times\frac{\tilde{\nu}_j\omega_B^2t_0^2(2E)}{4(1-\nu_j^2)\left\{\nu_j(1+\tilde{\nu}_j^2)-\tilde{\nu}_j\left[2+\left(\frac{F_2}{F_1}\right)^2(1-\nu_j^2)\right]\right\}}. \quad (42)$$

This gives the classical density at the origin for the jth orbit.

5. The Maslov index

The Maslov index μ_j is the number of caustics and foci through which the jth closed orbit passes, and caustics and foci are singular points where the Jacobian $J(t)$ goes to zero. Equation (34) shows that the Jacobian for the jth closed orbit depends upon $\sin(t/2)$, so we deduce that $J(t)$ goes to zero when $t=2k\pi$, with t less than or equal to $t_{\rm ret}$ (k is an integer). As $t=2k\pi$ is a multiple of the cyclotron time, the electron passes through a focus. The Jacobian $J(t)$ is also zero when

$$\tan\frac{t}{2}=\frac{t(\varepsilon_j-P_{y_0}-\frac{1}{2})}{\left[\left(\frac{F}{F_1}\right)^2t-\frac{1}{2}\left(\frac{F_2}{F_1}\right)^2t_{\rm ret}\right][2\varepsilon_j-(P_{y_0}+1)^2]^{1/2}}. \quad (43)$$

Solutions of Eq. (43) are times at which the electron passes through caustics.

Given the total energy E, which is larger than the boundary energies, there are two closed orbits for each j of Eq. (28), which are labeled by $j(a)$ and $j(b)$, respectively. The number of caustics and foci can be counted from the closed orbits (Figs. 3–7). We are able to conclude that the closed orbit $j(a)$ passes through $(2j+1)$ caustics and foci, while the closed orbit $j(b)$ passes through $2j$ caustics and foci.

6. The classical action

The classical action $s(q)$ is given by the following integral from the initial point q_0 to the final point q:

$$s(q)=\int_{q_0}^{q}\vec{p}\cdot d\vec{q}=\int_{q_0}^{q}\vec{p}\cdot\frac{d\vec{q}}{dt}dt. \quad (44)$$

TABLE I. The boundary energies from $j=1$ to 6 for three different values of the angle α.

	$\alpha=5°$				$\alpha=45°$				$\alpha=85°$			
Boundary orbit j	$E^{(b_j)}$ (scaled units)	$E^{(b_j)}$ (10^{-5} a.u.)	$\varepsilon^{(b_j)}$ (scaled units)	$\varepsilon^{(b_j)}$ (10^{-5} a.u.)	$E^{(b_j)}$ (scaled units)	$E^{(b_j)}$ (10^{-5} a.u.)	$\varepsilon^{(b_j)}$ (scaled units)	$\varepsilon^{(b_j)}$ (10^{-5} a.u.)	$E^{(b_j)}$ (scaled units)	$E^{(b_j)}$ (10^{-5} a.u.)	$\epsilon^{(b_j)}$ (scaled units)	$\varepsilon^{(b_j)}$ (10^{-5} a.u.)
1	830.0	1.185	76.31	0.1089	18.53	1.74	11.96	1.123	9.72	1.81	11.10	2.0669
2	3043.0	4.345	183.11	0.2614	57.84	5.431	32.21	3.0245	29.59	5.510	30.90	5.754
3	6599.65	9.4224	304.128	0.4342	116.98	10.984	61.59	5.7834	59.5	11.079	60.52	11.269
4	11481.0	16.391	447.21	0.6384	195.83	18.388	101.31	9.5131	99.23	18.478	99.95	18.612
5	17691.0	25.2576	594.38	0.8486	294.53	27.657	150.66	14.147	149.01	27.747	149.35	27.811
6	25241.0	36.0368	761.72	1.0875	413.0	38.781	210.1	19.728	208.65	38.853	208.55	38.835

Since $s(q_0)$ is an arbitrary factor, we take it to be zero. Using Eqs. (8) and (18), we calculate the integral in Eq. (44) and obtain the classical action in the following way:

$$s(E)=s(t_{\rm ret})=-\frac{1}{\omega_B}\left[\frac{F_1}{\omega_B}\right]^2\frac{1}{\tilde{\nu}_j^2}(1-\nu_j^2)^{1/2}\left[\nu_j-\frac{1}{\tilde{\nu}_j}\right]. \tag{45}$$

This is the classical action for the jth closed orbit.

III. PHOTODETACHMENT CROSS SECTION

Using the results of the preceding sections, we obtain the oscillatory part of the photodetachment cross section $\sigma_{\rm ret}$ in electric and magnetic fields with any orientations

$$\begin{aligned}\sigma_{\rm ret}=\sigma_0\sum_j&\left[\frac{6\omega_B}{F_1/\omega_B}\right]\frac{\pi}{\sqrt{2E}}\\&\times\left|\frac{\tilde{\nu}_j^2}{(1-\nu_j^2)\left\{\nu_j(1+\tilde{\nu}_j^2)-\tilde{\nu}\left[2+\left(\frac{F_2}{F_1}\right)^2(1-\nu_j^2)\right]\right\}}\right|^{1/2}\\&\times[\chi(\theta^j_{\rm out},\phi^j_{\rm out})\chi^*(\theta^j_{\rm ret},\phi^j_{\rm ret})]\\&\times\sin\left[\frac{1}{\omega_B}\left(\frac{F_1}{\omega_B}\right)^2\frac{1}{\tilde{\nu}_j^2}(1-\nu_j^2)^{1/2}\left(\nu_j-\frac{1}{\tilde{\nu}_j}\right)+\mu_j\frac{\pi}{2}\right].\end{aligned} \tag{46}$$

Let $\{\theta^k_{\rm ret},\phi^k_{\rm ret}\}$ represent the direction of motion of the returning electron at $t=t_{\rm ret}$, and $\{\theta^j_{\rm ret},\phi^j_{\rm ret}\}$ be the direction from which the electrons come. The relationship of $\{\theta^k_{\rm ret},\phi^k_{\rm ret}\}$ and $\{\theta^j_{\rm ret},\phi^j_{\rm ret}\}$ is [6]

$$\theta^k_{\rm ret}=\pi-\theta^j_{\rm ret},$$

$$\phi^k_{\rm ret}=\pi+\phi^j_{\rm ret}. \tag{47}$$

From Eqs. (8) and (18), we obtain that the initial momenta $\{P_{x_0},P_{y_0},P_{z_0}\}$ at $t=t_0$ and the final momenta $\{P_x(t_{\rm ret}),P_y(t_{\rm ret}),P_z(t_{\rm ret})\}$ at $t=t_{\rm ret}$ can be expressed in the following way:

$$P_{x_0}=\sqrt{2E}\,\sin\theta^j_{\rm out}\cos\phi^j_{\rm out},$$

$$P_{y_0}=\sqrt{2E}\,\sin\theta^j_{\rm out}\sin\phi^j_{\rm out},$$

$$P_{z_0}=\sqrt{2E}\,\cos\theta^j_{\rm out}, \tag{48a}$$

and

$$P_x(t_{\rm ret})=\sqrt{2E}\,\sin\theta^k_{\rm ret}\cos\phi^k_{\rm ret}=-P_{x_0},$$

$$P_y(t_{\rm ret})=\sqrt{2E}\,\sin\theta^k_{\rm ret}\sin\phi^k_{\rm ret}=P_{y_0},$$

$$P_z(t_{\rm ret})=\sqrt{2E}\cos\theta^k_{\rm ret}=-P_{z_0}. \tag{48b}$$

Therefore, from Eqs. (26), (47), and (48) we give the relationship between $\{\theta^j_{\rm out},\phi^j_{\rm out}\}$ and $\{\theta^j_{\rm ret},\phi^j_{\rm ret}\}$,

$$\theta^j_{\rm out}=\theta^j_{\rm ret}=\alpha,$$

$$\phi^j_{\rm out}=-\phi^j_{\rm ret}. \tag{48c}$$

With the help of Eqs. (47) and (48), we write for various linear polarizations

$$\chi_x(\theta^j_{\rm out},\phi^j_{\rm out})\chi_x^*(\theta^j_{\rm ret},\phi^j_{\rm ret})=\frac{1}{4\pi}\sin^2\theta^j_{\rm out}\cos^2\phi^j_{\rm out},$$

$$\chi_y(\theta^j_{\rm out},\phi^j_{\rm out})\chi_y^*(\theta^j_{\rm ret},\phi^j_{\rm ret})=-\frac{1}{4\pi}\sin^2\theta^j_{\rm out}\sin^2\phi^j_{\rm out},$$

$$\begin{aligned}\chi_z(\theta^j_{\rm out},\phi^j_{\rm out})\chi_z^*(\theta^j_{\rm ret},\phi^j_{\rm ret})&=\frac{1}{4\pi}\cos^2\theta^j_{\rm out}\\&=\frac{1}{4\pi}\left(\frac{F_2}{F_1}\right)^2\sin^2\theta^j_{\rm out}\cos^2\phi^j_{\rm out}.\end{aligned} \tag{49a}$$

Coming out of the scaled variables and using Eq. (48) and the dimensionless variables defined by Eq. (41), we rewrite Eq. (49a) in $\tilde{\nu}_j$, and ν_j,

$$\chi_x(\theta^j_{\rm out},\phi^j_{\rm out})\chi^*_x(\theta^j_{\rm ret},\phi^j_{\rm ret})=\frac{1}{4\pi}\left(\frac{F_1}{\omega_B}\right)^2\frac{1}{2E}\frac{1-\nu_j^2}{\tilde{\nu}_j^2},$$

$$\chi_y(\theta^j_{\rm out},\phi^j_{\rm out})\chi^*_y(\theta^j_{\rm ret},\phi^j_{\rm ret})=-\frac{1}{4\pi}\left(\frac{F_1}{\omega_B}\right)^2\frac{1}{2E}\frac{(\nu_j-\tilde{\nu}_j)^2}{\tilde{\nu}_j^2},$$

$$\chi_z(\theta^j_{\rm out},\phi^j_{\rm out})\chi^*_z(\theta^j_{\rm ret},\phi^j_{\rm ret})=\frac{1}{4\pi}\left(\frac{F_1}{\omega_B}\right)^2\left(\frac{F_2}{F_1}\right)^2\frac{1}{2E}\frac{1-\nu_j^2}{\tilde{\nu}_j^2}. \tag{49b}$$

Finally, we calculate the photodetachment cross section for x-polarized light in the following way:

$$(2E)^{3/2}\left|\frac{\sigma_x-\sigma_0}{\sigma_0}\right|=\sum_j c_j^x(E)\sin[\Phi_j(E)], \tag{50a}$$

where $c_j^x(E)$ is given by

$$c_j^x(E)=\frac{3}{2}\frac{F_1}{\tilde{\nu}_j}\left|\frac{\tilde{\nu}_j(1-\nu_j^2)}{\nu_j(1+\tilde{\nu}_j^2)-\tilde{\nu}_j\left[2+\left(\frac{F_2}{F_1}\right)^2(1-\nu_j^2)\right]}\right|^{1/2}. \tag{50b}$$

Similar equations hold for y- or z- polarized light, and $c_j^y(E)$ and $c_j^z(E)$ are

$$c_j^y(E)=\frac{3}{2}\frac{F_1}{\tilde{\nu}_j}\left|\frac{\tilde{\nu}_j(1-\nu_j^2)}{\nu_j(1+\tilde{\nu}_j^2)-\tilde{\nu}_j\left[2+\left(\frac{F_2}{F_1}\right)^2(1-\nu_j^2)\right]}\right|^{1/2}\times\frac{(\nu_j-\tilde{\nu}_j)^2}{(1-\nu_j^2)^{1/2}}, \tag{50c}$$

$$c_j^z(E)=\frac{3}{2}\left[\frac{F_2}{F_1}\right]^2\frac{F_1}{\tilde{\nu}_j}\times\left|\frac{\tilde{\nu}_j(1-\nu_j^2)}{\nu_j(1+\tilde{\nu}_j^2)-\tilde{\nu}_j\left[2+\left(\frac{F_2}{F_1}\right)^2(1-\nu_j^2)\right]}\right|^{1/2}. \tag{50d}$$

We have removed the cross section σ_0 in the absence of fields and kept only the oscillatory part of the spectrum. Dividing by σ_0 and multiplying by the factor $(2E)^{3/2}$ does not change the nature of the oscillations, but only changes the amplitude.

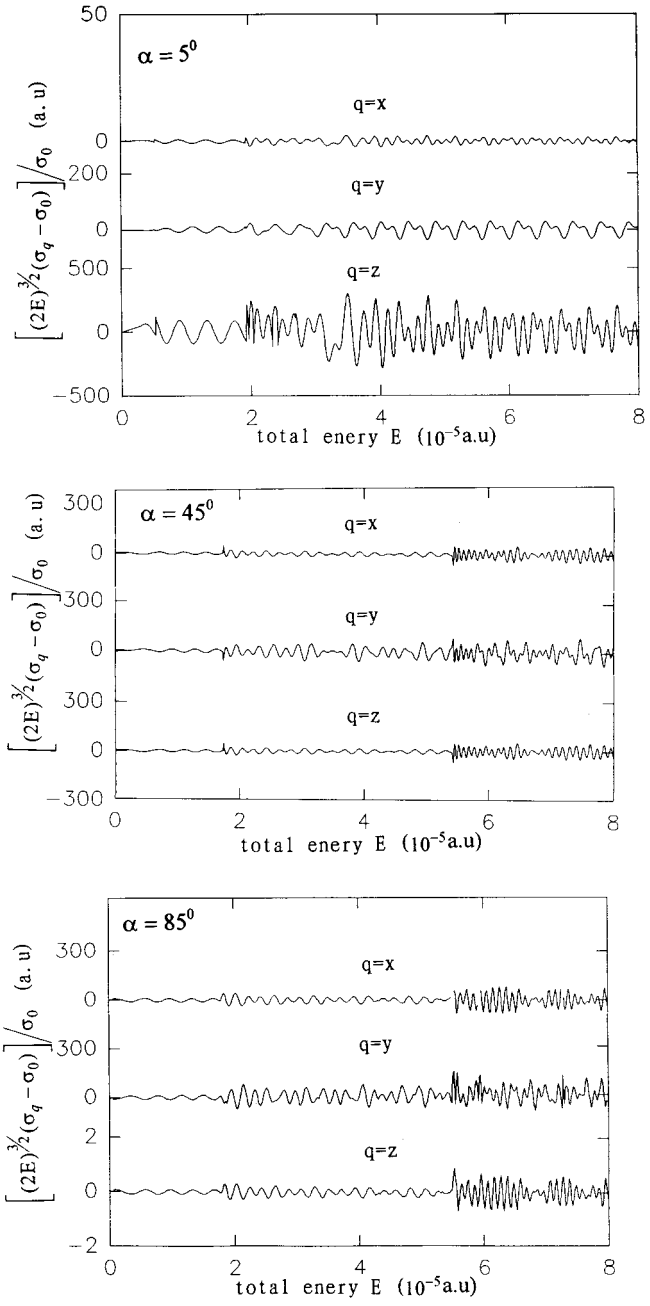

FIG. 10. With light linearly polarized in the x, y, or z directions, the semiclassical oscillations of the photodetachment cross sections are displayed. For x- or z-polarized light, the amplitude of the oscillations decreases with increasing energy, while for y-polarized light, it increases. As the value of the angle α becomes small, for x or y-polarized light, the amplitude of oscillations decreases, while for z-polarized light, the amplitude increases. As α tends to zero, the amplitude of the z-polarized light increases sharply.

Evaluation of the semiclassical cross section for the parameters shown in Fig. 10 is given in the following process: First, we find out the number of the closed orbits for any

given energy E by solving Eq. (28). The total scaled energy is given by

$$E' = \left[\frac{F_1}{\omega_B}\right]^{-2} E. \tag{51}$$

So from Table I, the number of the closed orbits can be determined easily. Second, for a given energy E, ε_j for each closed orbit is calculated by solving Eq. (28). With ε_j known, P_j (or P_{y_0}) for that closed orbit can be evaluated by Eq. (29). Then two dimensionless quantities $\tilde{\nu}_j$ and ν_j can be determined by Eq. (41), and the photodetachment cross section can be calculated.

Following the preceding process of calculation, the right-hand side of Eq. (50a) is calculated for the range of atomic energies $0.0–8.0\times10^{-5}$ a.u. The results are shown in Fig. 10.

IV. SIMILARITIES AND DIFFERENCES BETWEEN THE CASE OF $\alpha=\pi/2$ and $\alpha\neq\pi/2$

For H^- in crossed electric and magnetic fields ($\alpha=\pi/2$), the classical motion of the detached electron has been obtained by Peters and Delos [1]. In that case, due to no electric field in the z axis for closed orbits, P_{z_0} must be zero. The closed orbits can exist only in the x-y plane. But in our case, the angle α between the electric and magnetic fields is less than $\pi/2$, the electric field $\vec{F}$ has one component F_2 in the z direction (Fig. 1), so for closed orbits P_{z_0} must be greater than zero. The closed orbits cannot exist in the x-y plane, except in three-dimensional space.

In our case of $\alpha\neq\pi/2$, calculations show that at any given energy E there is at least one closed orbit, and there is a set of boundary energies $E^{(b_j)}$. At each boundary energy $E^{(b_j)}$, a new closed orbit is created, and with the slightest increase of energy, the newly created closed orbit separates into two closed orbits, labeled by $j(a)$ and $j(b)$, respectively. Each closed orbit is described by a parameter [$\varepsilon_j(a)$ and $\varepsilon_j(b)$, and with $\varepsilon_j(a)<\varepsilon_j(b)$], which represents the circular kinetic energy of the electron's trochoidal motion in the x-y plane. For any given energy E, other than the boundary energies, the number of closed orbits is $(2j+1)$ (Table I). The Maslov index μ_j is $(2j+1)$ for the $j(a)$ orbit, while it is $2j$ for the $j(b)$ orbit. These results are the same as those obtained by Peters and Delos [1] in the case of $\alpha=\pi/2$. Our calculations also show that the jth boundary energy $E^{(b_j)}$ reduces with a decreasing value of angle α (Fig. 9 and Table I). As the value of α tends to zero, the boundary energy $E^{(b_j)}$ decreases sharply, approaching the boundary energy in parallel electric and magnetic fields [2]. Therefore, for a given energy E, there may be more closed orbits for the smaller value of angle α. This fact is shown clearly in Table I. More closed orbits can give rise to more complicated oscillations in the cross-section spectrum.

For three different values of angle α, Fig. 10 gives the oscillatory parts of the photodetachment cross sections for linearly polarized light on the x, y, or z axis. For a given value of angle α, the amplitude of the oscillations for x-polarized light is largest near the boundary energy and then decreases with increasing energy, while the amplitude for y-polarized light increases with increasing energy. An explanation of these facts can be given in the following way. Equation (49a) shows that for x-polarized light the amplitude is proportional to $\sin^2\theta^{\,j}_{\rm out}\cos^2\phi^{\,j}_{\rm out}$, while for y-polarized light it is proportional to $\sin^2\theta^{\,j}_{\rm out}\sin^2\phi^{\,j}_{\rm out}$. Equation (48c) displays that the angular factor $\theta^{\,j}_{\rm out}$ is equal to the angle α. So for a given value of angle α, the angular factor $\theta^{\,j}_{\rm out}$ is a constant and then cannot change the amplitude with increasing energy. However, the angular factor $\phi^{\,j}_{\rm out}$ is at a minimum at the boundary energy $E^{(b_j)}$, and then increases as the energy increases away from $E^{(b_j)}$. Then the amplitude for x-polarized light decreases, while the amplitude for y-polarized light increases. The amplitude for z-polarized light is the multiplication of the one for x-polarized light by a factor $(F_2/F_1)^2$ [Eq. (49a)], and they have similar changing tendencies with increasing energy. The only difference is that their oscillations have different amplitudes.

In the case of $\alpha=\pi/2$, the photodetachment cross section for x or y-polarized light is similar to the case of $\alpha\neq\pi/2$, but for z-polarized light, the cross sections for two cases ($\alpha=\pi/2$ and $\alpha\neq\pi/2$) are different. At $\alpha=\pi/2$, the oscillatory cross section for z-polarized light is equal to zero. This is because the closed orbits lie only in the x-y plane, and with z-polarized light there is no outgoing wave in the x-y plane [Eq. (4.2) in Ref. [1]]. Thus, the closed orbits have no influence and the cross section has no oscillations. As the value of angle α reduces away from $\alpha=\pi/2$, the closed orbits cannot exist in the x-y plane, except in three-dimensional space. Therefore, though there is no outgoing wave in the x-y plane, the closed orbits still have an effect on the cross section, giving rise to the oscillations in the cross section. At $\alpha\neq\pi/2$, Eq. (49a) shows that the amplitude of the oscillations for z-polarized light is proportional to $\cos^2\theta^{\,j}_{\rm out}$, and the angular factor $\theta^{\,j}_{\rm out}$ is equal to the angle α; so, as the value of angle α decreases, the angular factor $\theta^{\,j}_{\rm out}$ decreases, and then the amplitude increases. As angle α approaches zero, the amplitude increases sharply.

The photodetachment cross section and other results of the case $\alpha=\pi/2$ given by Peters and Delos [1] can be obtained easily from the results in this paper just by taking $\alpha\rightarrow\pi/2$ or $F_2\rightarrow0$. But the results of the case $\alpha=0$ given by Peters *et al.* [2] cannot be obtained directly from our results just by taking $\alpha\rightarrow0$ or $F_1\rightarrow0$. This is due to the following cause. In parallel electric and magnetic fields ($\alpha=0$), the forces acting on the detached electron are cylindrically symmetric. So, each closed orbit given in Ref. [2] actually represents a cylindrical family of orbits and the number of closed orbits is infinite. However, in our case ($0<\alpha<\pi/2$), this symmetry does not exist, so each closed orbit is isolated, and the number of closed orbits is finite. As $\alpha\rightarrow0$, the evolution of our results to the case of $\alpha=0$ needs to be studied further. This is planned for the future.

ACKNOWLEDGMENT

We especially thank M. L. Du for many helpful discussions and suggestions.

[1] A. D. Peters and J. B. Delos, Phys. Rev. A **47**, 3020 (1993); **47**, 3036 (1993).
[2] A. D. Peters, C. Jaffe, and J. B. Delos, Phys. Rev. Lett. **73**, 2825 (1984).
[3] M. L. Du, Phys. Rev. A **40**, 1330 (1989).
[4] M. L. Du and J. B. Delos, Phys. Rev. Lett. **58**, 1731 (1987); Phys. Rev. A **38**, 5609 (1988); M. L. Du, Phys. Lett. A **134**, 476 (1989); A. R. P. Rau and H. Y. Wong, Phys. Rev. A **37**, 632 (1988).
[5] John David Jackson, *Classical Electrodynamics*, 2nd. ed. (Wiley, New York, 1975), pp. 582–584.
[6] M. L. Du and J. B. Delos, Phys. Rev. A **38**, 1913 (1988); **38**, 1986 (1988).